

See discussions, stats, and author profiles for this publication at: <https://www.researchgate.net/publication/274642935>

Topical treatment with pterostilbene, a natural phytoalexin, effectively protects hairless mice against UVB radiation-induced skin damage and carcinogenesis

Article in *Free Radical Biology and Medicine* · April 2015

DOI: 10.1016/j.freeradbiomed.2015.03.027 · Source: PubMed

CITATIONS

111

READS

1,858

10 authors, including:



Joan Antoni Sírerol

University of Valencia

17 PUBLICATIONS 529 CITATIONS

[SEE PROFILE](#)



Salva Mena

University of Valencia

29 PUBLICATIONS 1,998 CITATIONS

[SEE PROFILE](#)



Miguel Aupí

University of Valencia

5 PUBLICATIONS 168 CITATIONS

[SEE PROFILE](#)



Salvador Pérez

University of Valencia

66 PUBLICATIONS 1,776 CITATIONS

[SEE PROFILE](#)



ELSEVIER

Contents lists available at ScienceDirect

Free Radical Biology and Medicine

journal homepage: www.elsevier.com/locate/freeradbiomed

Original Contribution

Topical treatment with pterostilbene, a natural phytoalexin, effectively protects hairless mice against UVB radiation-induced skin damage and carcinogenesis



J. Antoni Sirerol^a, Fatima Feddi^b, Salvador Mena^a, María L. Rodríguez^a, Paula Sirera^a, Miguel Aupí^a, Salvador Pérez^a, Miguel Asensi^{a,b}, Angel Ortega^{a,b}, José M. Estrela^{a,b,*}

^a Department of Physiology, University of Valencia, 46010 Valencia, Spain

^b Green Molecular S.L., Scientific Park, University of Valencia, Paterna, Spain

ARTICLE INFO

Article history:

Received 15 January 2015

Received in revised form

19 March 2015

Accepted 25 March 2015

Available online 4 April 2015

Keywords:

Phytochemicals

Polyphenols

Stilbenes

Pterostilbene

Resveratrol

UV radiation

Photocarcinogenesis

Skin damage

Oxidative stress

Free radicals

ABSTRACT

The aim of our study was to investigate in the SKH-1 hairless mouse model the effect of pterostilbene (Pter), a natural dimethoxy analog of resveratrol (Resv), against procarcinogenic ultraviolet B radiation (UVB)-induced skin damage. Pter prevented acute UVB (360 mJ/cm²)-induced increase in skin fold, thickness, and redness, as well as photoaging-associated skin wrinkling and hyperplasia. Pter, but not Resv, effectively prevented chronic UVB (180 mJ/cm², three doses/week for 6 months)-induced skin carcinogenesis (90% of Pter-treated mice did not develop skin carcinomas, whereas a large number of tumors were observed in all controls). This anticarcinogenic effect was associated with (a) maintenance of skin antioxidant defenses (i.e., glutathione (GSH) levels, catalase, superoxide, and GSH peroxidase activities) close to control values (untreated mice) and (b) an inhibition of UVB-induced oxidative damage (using as biomarkers 8-hydroxy-2'-deoxyguanosine, protein carbonyls, and isoprostanes). The molecular mechanism underlying the photoprotective effect elicited by Pter was further evaluated using HaCaT immortalized human keratinocytes and was shown to involve potential modulation of the Nrf2-dependent antioxidant response.

© 2015 Elsevier Inc. All rights reserved.

Introduction

Solar radiation exposure is the chief cause of nonmelanoma (i.e., basal cell and squamous cell) skin cancer, and it is also a prime factor in the etiology of cutaneous melanoma [1]. The cancer-causing effects of ultraviolet (UV) radiation on the skin are mainly produced by UVB radiation in the 290- to 320-nm range, the same range that produces burning in human skin (erythema) [2]. UVB exposure can damage DNA and be immunosuppressive [3]. Thus, considering the alarming numbers of skin cancers being diagnosed around the world, it is increasingly evident that there is a need for effective protection from UV radiation (www.skincancer.org).

Abbreviations: Pter, pterostilbene; Resv, resveratrol; GSH, glutathione; PMMA, polymethylmethacrylate; SPF, sun protection factor; CAT, catalase; SOD, superoxide dismutase; GPX, glutathione peroxidase; Nrf2, nuclear factor erythroid-2-related factor-2; γ-GCL, γ-glutamyl-cysteine ligase; Trx, thioredoxin; ROS, reactive oxygen species; DFO, desferrioxamine; DFP, deferiprone

* Corresponding author at: Department of Physiology, University of Valencia, 46010 Valencia, Spain. Fax: +34 963864642.

E-mail address: jose.m.estrela@uv.es (J.M. Estrela).

Phytochemicals with polyphenolic structure, such as those isolated from green tea, pomegranate, and grape seed, have shown potent antioxidant properties and potential benefits in a variety of human diseases, including cancer [4,5]. Thus these molecules represent an interesting avenue of research as additives to sunscreens or stand-alone products that may modulate the immunosuppressive and procarcinogenic effects of UV radiation on the skin [6–8].

The cancer chemopreventive activity of resveratrol (*trans*-3,5,4'-trihydroxystilbene; Resv)¹, a phytoalexin present in a wide variety of plant species, in which its synthesis is induced by stress conditions, was first reported by Jang et al. [9] in a model of skin carcinogenesis in which topical administration of this stilbene inhibited multistage mouse skin carcinogenesis. Later, Resv showed remarkable cancer chemopreventive effects in a variety of tumor bioassay models (e.g., [10]).

Equally promising action is exerted by the resveratrol analog pterostilbene (3,5-dimethoxy-4'-hydroxy-*trans*-stilbene; Pter), which shows a longer half-life in vivo and even more potent anticancer effects than Resv [11]. For instance, when Pter and Resv were compared, Pter was found to be more potent than Resv in preventing azoxymethane-induced colon tumorigenesis [12]. Pter also showed a higher anti-inflammatory activity than Resv [13], a fact particularly

relevant because inflammation, gene mutation, and photoimmunosuppression in response to UV radiation contribute to photocarcinogenesis [14].

Pterostilbene has a more favorable pharmacokinetic profile [15–17]. Pter contains two methoxy groups and one hydroxyl group, whereas Resv has three hydroxyl groups; in consequence Pter is less susceptible to conjugation metabolism and, thus, a longer half-life is expected [18,19]. The dimethoxy structure of Pter enhances its lipophilicity, thus increasing membrane permeability and improving its bioavailability [11,16,18,20]. Nevertheless, it is uncertain whether the chemical differences between Resv and Pter may represent a fundamental difference in terms of protection against chronic UVB-induced skin carcinogenesis. Thus, and thinking of the close relationship between cumulative UVB radiation dose and skin damage, we compared the potential photoprotective effects of Pter and Resv at various time steps. Our results show that Pter, but not Resv, exerts full protection in most treated animals (90%). Pter effectively prevents chronic UVB-induced oxidative damage, in which modulation of Nrf2 activity seems to be involved in the underlying mechanism.

Materials and methods

Animals

Female SKH-1 hairless mice (10–12 weeks of age) from Charles River Laboratories International (Wilmington, MA, USA) were fed ad libitum on a standard diet (Leticia, Barcelona, Spain). Mice were kept on a 12-h light/12-h dark cycle with the room temperature kept at 22 °C. Procedures involving animals were in compliance with international laws and policies (EEC Directive 86/609, OJ L 358.1, December 12, 1987, and NIH *Guide for the Care and Use of Laboratory Animals*, NIH Publication No. 85–23, 1985).

Stilbenes and liposomes preparation for topic administration

The methodology of preparation of liposomes was as follows: (a) Stilbene (0.512 g of Pter (Green Molecular, Paterna, Spain) or 0.676 g of Resv (Sigma–Aldrich, St. Louis, MO, USA)) and lecithin (2.376 g (Guinama, Alboraya, Valencia, Spain)) were dissolved in 40 ml of dichloromethane (Sigma–Aldrich) (in the case of Pter) or 140 ml of ethyl ether (Sigma–Aldrich) (in the case of Resv). (Pter and Resv exist as two geometric isomers, *cis* and *trans*, but naturally occurring structures overwhelmingly exist in the *trans* form. Thus both commercially available stilbenes were corresponded to their *trans* form, > 99%.) (b) The solution was introduced into a rotary evaporator flask and attached to the device (Büchi Labortechnik AG, Switzerland). The evaporation of organic solvent was performed at 40 °C. Once all the solvent evaporated the expected vacuum was cut and 15 min was allowed to eliminate all traces of solvent that may have remained. (c) Diluted phosphate-buffered saline (PBS; 1 mM, 20 ml) was added to the rotary evaporator flask and the device was reattached but this time without vacuum. (d) The liposomes formed were collected in a 50-ml tube. (e) The liposomes were sonicated (6 s, 25 cycles, with an interval of 3 s between each cycle; high intensity) using a Soniprep 150 (MSE Ltd., London, UK). (f) The samples were diluted 1:1 with Carbopol (Guinama; final concentration 10 µmol/200 µl). (Before the Carbopol was added, the concentration of each polyphenol was 20 µM as determined by LC–MS/MS.) (g) Phenonip was added to avoid contamination (Guinama; 6 ml of Phenonip per 1000 ml of preparation) [21]. Control liposomes were made in the same manner as those of Pter or Resv, but contained only lecithin.

Antioxidant capacity

To measure the antioxidant activity of each compound we used the Trolox (a vitamin E derivative, Sigma–Aldrich) method [22], which is based on the reaction between H₂O₂ and metmyoglobin to form ferryl myoglobin. This radical reacts with ABST (2,2'-azino-bis(3-ethylbenzothiazoline-6-diammonium sulfonate)) (Sigma–Aldrich) to form ABST^{•+}, a chromogen that presents a peak of absorbance at 734 nm. In the presence of potential antioxidants, such as Pter or Resv, there is an inhibition of that absorbance, which is used to determine their antioxidant capacity. As a calibration curve various concentrations of Trolox were used.

UV absorption and SPF determination

Standard solutions of stilbenes were prepared to 1 mM in ethanol. The absorption was measured with a Multiskan Spectrum (ThermoScientific, Waltham, MA, USA) at a scan range of 200–800 nm. The blank used was ethanol.

Determination of the sun protection factor (SPF), by means of a spectrophotometer, was based on the method described by Diffey and Robson [23] and then modified and improved with the view to evaluate the skin protection against UV brought by the product. The *in vitro* method described in this report allows one to reach the same value by means of a spectrophotometric measurement of the residual spectrum having crossed the spread product, and it is completed by a mathematical adjustment as proposed by Diffey and Robson [23]. As a substrate, the material to which the sun care product was applied, the polymethylmethacrylate (PMMA) plates named Helioplate HD6 (HelioScreen, Creil, France), was to guarantee the correct roughness.

Deposit is best done as small lined-up spots all over the surface. As deposited on the substrate, product quantity was checked by weighing. Application rate was determined in such a way that the quantity of product left on the substrate before equilibration was 1.3 mg/cm². To ensure accuracy, the application area was about 25 cm². As soon as the correct quantity had been deposited, the product was immediately spread over the whole substrate surface using a gloved or bare finger, until a uniform film was achieved. This spreading was completed as quickly as possible and spreading uniformity was carefully checked. The samples thus obtained were allowed to equilibrate for 15 min in the dark at room temperature to ensure a self-leveling of the formula.

A PMMA plate containing a UV filter was used as a reference so as to check that the equipment was in good working order and to assess the relevance of carried out measures.

The *in vitro* SPF is expressed from the whole residual UVB and UVA spectrum having crossed the cream layer spread on the substrate. This leads to a wave function $T(\lambda)$, which was multiplied by:

- a first wave function $S(\lambda)$, spectral irradiance of the standard sun;
- a second wave function $E(\lambda)$, erythemal action spectrum.

The SPF was calculated from the following ratio:

$$SPF \text{ in vitro} = \frac{\sum_{290}^{400} E(\lambda) \cdot S(\lambda) \cdot d\lambda}{\sum_{290}^{400} E(\lambda) \cdot S(\lambda) \cdot T(\lambda) \cdot d\lambda}$$

The SPF values of tested products were obtained by calculating the arithmetical average of the different measures: all measures corresponding to selected samples were taken into account for the calculation of the statistical dispersion. For calculations, the Heliosoft Ltd. (Buckinghamshire, UK) software was used.

UVB irradiation, treatment with liposomes, mouse sacrifice, and tissue sample processing

Mice were irradiated with UVB (acute exposure, one irradiation of 360 mJ/cm²; chronic exposure, 180 mJ/cm², 3 doses/week for a total of 30 weeks) 20 min after or before the topical administration of liposomes (empty or containing 1–2 μmol Pter or Resv/cm² of skin) [24,25]. UVB irradiation was performed using a Crosslinker Bio-Link BLX 254 camera (5 × 8 W; Peqlab Biotechnologie GmbH, Erlangen, Germany) and a wavelength of 310 nm. The long-term exposure protocol reproduces, in an animal model, the consequences expected in humans receiving chronic UVB radiation.

After treatment mice were sacrificed, at the time points indicated under Results, using difluoromethane and cervical dislocation. Skin was rapidly separated and used for histopathology studies (skin samples were fixed with 4% paraformaldehyde in PBS, pH 7.4, and then dehydrated and paraffin embedded) or enzyme activity and gene expression measurements (skin samples were frozen with liquid nitrogen and kept at –80 °C until further processing). Plasma samples of each sacrificed mouse were also collected in heparinized Eppendorf tubes (ROVI Laboratories, Madrid, Spain).

Skin samples from the –80 °C storage were homogenized at 0 to –10 °C using a Precellys 24 homogenizer (Bertin Technologies, Montigny-le-Bretonneux, France) coupled to a Cryolys system (Bertin Technologies) (six cycles of shaking at 6300 rpm, 23 s/cycle). This procedure facilitates a perfect homogenization.

Protein determination

Protein levels in skin homogenates were measured using the Pierce BCA protein assay kit (Thermo Scientific, Erembodegem, Belgium) and following the manufacturer's protocol.

Skin thickness measurement

Skin thickness, as a parameter of UVB-induced skin edema, was measured using electronic calipers (MEDID, General de Medición, S.L., Barcelona, Spain) [26]. This value was expressed as the percentage of skin thickness increase compared to controls: ((skin thickness 24 h after irradiation – skin thickness before irradiation)/skin thickness before irradiation) × 100. Hematoxylin and eosin staining of skin samples, fixed with 4% paraformaldehyde and paraffin embedded, was used to determine the epidermis thickness using the open software ImageJ. The number of epidermal cell layers was also calculated.

Quantitative determination of iron

A Spinreact (San Esteve de Bas, Spain) standard methodology was used in which the iron was dissociated from the transferrin–iron complex in weakly acid medium. Liberated iron is reduced into the bivalent form by means of ascorbic acid. Ferrous ions treated with FerroZine give a colored complex (measured spectrophotometrically at 562 nm) (method sensitivity is 10 ng/ml).

Measurement of pterostilbene and its metabolites

For this purpose skin samples were homogenized in PBS using a Precellys 24 homogenizer. Aliquots of 100 μl of plasma or supernatant of skin samples homogenized in PBS were directly mixed with 200 μl of cool methanol. Then samples were centrifuged at 10,000 g for 15 min, at 4 °C, using a Mikro 200 R centrifuge (Andreas Hettich, Tuttlingen, Germany). The supernatants were directly used for Pter determination. UPLC–MS/MS was carried out according to Ferrer et al. [27], using an Acquity

UPLC system with triple-quadrupole mass spectrometer (Waters Corp., Milford, MA, USA). Pter metabolites were identified in a full-scan mode.

GSH determination

GSH was determined by liquid chromatography coupled with tandem mass spectrometry (Acquity UPLC system with triple-quadrupole mass spectrometer (Waters)) following the Escobar et al. procedure [28]. Before homogenization, 10 mM *N*-ethylmaleimide was added to each skin sample. Samples were deproteinized with 4% v/v perchloric acid and centrifuged at 10,000 g for 15 min at 4 °C. The supernatants were directly used for GSH determination. The results were corrected for the number of cell layers measured in the epidermis for each condition.

Lipid peroxidation

For isoprostane determination skin samples, stored at –80 °C, were homogenized (see above) in 0.1 M phosphate buffer (pH 7.4)+1 mM EDTA+0.005% butylated hydroxytoluene. Isoprostanes were measured using the 8-isoprostane EIA kit (Cayman Chemical, Ann Arbor, MI, USA) and following the manufacturer's protocol.

Protein carbonylation

Carbonylation of proteins, an irreversible oxidative damage, was measured using the OxyBlot Protein Oxidation Detection Kit (EMD Millipore Corp., Billerica, MA, USA) and following the manufacturer's protocol.

DNA damage

Skin samples were homogenized in 10 mM Tris (pH 7.0)+1 mM EDTA+150 mM NaCl. Thereafter they were incubated first with RNase A at 37 °C for 30 min and then with proteinase K at 55 °C overnight. This was followed by chloroform/isoamyl alcohol extraction. Samples of 100 μg of isolated DNA were digested to nucleosides with nuclease P1 and alkaline phosphatase [29]. Analysis of modified DNA base 8-hydroxy-2'-deoxyguanosine (8-OHdG) was accomplished by UPLC–MS/MS.

Enzyme activities

Skin samples from the –80 °C storage were homogenized, at 4 °C, in 50 mM potassium phosphate (pH 7.0)+ 1 mM EDTA (for CAT, catalase determination), in 20 mM Hepes (pH 7.2)+1 mM EGTA+210 mM mannitol+70 mM sucrose (for SOD, superoxide dismutase determination), or in 50 mM Tris–HCl (pH 7.5)+5 mM EDTA+1 mM dithiothreitol (DTT) (for GPX, glutathione peroxidase determination). Homogenates were centrifuged at 10,000 g for 15 min, at 4 °C, using a Mikro 200 R centrifuge. The supernatants were directly used for enzyme activity determination. CAT, SOD, and GPX activities were determined using the Catalase Assay Kit, the Superoxide Dismutase Assay Kit, and the Glutathione Peroxidase Assay Kit (Cayman), respectively, following the manufacturer's protocols.

RT-PCR

Total RNA was isolated using the TRIzol kit from Invitrogen following the manufacturer's instructions. cDNA was obtained using a random hexamer primer and a MultiScribe reverse transcriptase kit as recommended by the manufacturer (TaqMan RT Reagents, Applied Biosystems, Foster City, CA, USA). PCR master

mix and AmpliTaq Gold DNA polymerase (Applied Biosystems) were added to the following primer sequences (5' to 3'): CAT, sense GGAGCAGGTGCTTTGGATA and antisense GAGGGTCAC-GAACTGTGTC; SOD1, sense TTTTTCGCGGTCTTTC and antisense CCATACTGATGGACGTGGAA; GPX, sense ATCAGTTCGGACACCAG-GAG and antisense TTCCGACGGAAGGTAAGAG. Real-time quantification of mRNA relative to GAPDH was performed with a SYBR Green I assay and an iCycler detection system (Bio-Rad, Hercules, CA, USA). Target cDNA was amplified using the following conditions: 10 min at 95 °C followed by 40 cycles of denaturation at 95 °C for 30 s and annealing and extension at 60 °C for 1 min. Changes in fluorescence were measured in real time during the extension step. The threshold cycle (C_T) was determined and the relative gene expression expressed as fold change = $2^{-\Delta(\Delta C_T)}$, where $\Delta C_T = C_{T \text{ target}} - C_{T \text{ GAPDH}}$, and $\Delta(\Delta C_T) = \Delta C_{T \text{ treated}} - \Delta C_{T \text{ control}}$.

HaCaT cell culture

Human immortalized keratinocytes (HaCaT cells, ATCC, Manassas, VA, USA) were cultured in Dulbecco's modified Eagle's medium, pH 7.4, supplemented with 4.5 g/L glucose, 2 mM L-glutamine, 10% heat-inactivated fetal bovine serum (Biochrom KG, Berlin, Germany), 100 units/ml penicillin, and 100 µg/ml streptomycin. Cells were plated at a density of 20,000 cells/cm² and cultured at 37 °C in a humidified atmosphere with 5% CO₂. Cells were harvested by incubation for 5 min with 0.05% (w/v) trypsin (Sigma) in PBS, pH 7.4, containing 0.3 mM EDTA, followed by the addition of 10% fetal calf serum to inactivate the trypsin. Cell numbers were determined using a Coulter Counter (Coulter Electronic, Miami, FL, USA). Cells were allowed to attach for 24 h before any treatment addition. Cellular viability was assessed by measuring trypan blue exclusion and leakage of lactate dehydrogenase activity.

Preparation of cytosolic and nuclear extracts

To prepare cytosolic and nuclear extracts cultured HaCaT cells were treated, 24 h after seeding, with Pter or control dimethyl sulfoxide. Three hours later HaCaT cell monolayers were dissociated with trypsin and centrifuged (525 g) for 2 min, at 4 °C. The supernatant was discarded and 1 ml of buffer A (10 mM HEPES, pH 7.9, 10 mM KCl, 1.5 mM MgCl₂, 5 µl/ml of Sigma's protease inhibitor, 1 mM DTT) was added to the pellet for resuspension by repeated pipetting. Then 62.5 µl of 10% Igepal was added to the cell suspension. After centrifugation, at 4 °C for 10 min at 3000 g, the supernatants were separated as "cytosolic extracts." The remaining pellet was washed with buffer A and, after centrifugation at 4 °C for 10 min at 3000 g, we added 125 µl of buffer B (20 mM HEPES, pH 7.9, 0.4 M NaCl, 1 mM EDTA, 1 mM EGTA, 5 µl/ml Sigma's protease inhibitor, 1 mM DTT). Then, after active shaking, the samples were centrifuged at 4 °C for 15 min at 12,000 g. The resulting supernatants were separated as "nuclear extracts" [30].

Western blots

For Western blotting, cultured cells, harvested as indicated above, or minced tissues were washed twice in ice-cold Krebs-Henseleit bicarbonate medium (pH 7.4). Cell or tissue extracts were made by freeze-thaw cycles (cells) or homogenization (tissues) in a buffer containing 150 mM NaCl, 1 mM EDTA, 10 mM Tris-HCl, 1 mM phenylmethylsulfonyl fluoride, 1 µg/ml leupeptin, 1 µg/ml aprotinin, and 1 µg/ml pepstatin (pH 7.4). About 50 µg of protein (as determined by the BCA assay) was boiled with Laemmli buffer and resolved in 12.5% SDS-PAGE.

Proteins were transferred to a nitrocellulose membrane and subjected to Western blotting with anti-human Nrf2, γ-glutamylcysteine synthetase (γ-GCL), or thioredoxin (Trx) monoclonal antibodies (Santa Cruz Biotechnology, Dallas, TX, USA). Blots were developed using horseradish peroxidase-conjugated secondary antibody and enhanced chemiluminescence (ECL system, Amersham). Protein bands were quantified using laser densitometry and Image Lab software (Bio-Rad). To make the pooling of data from different immunoblots possible, the relative density of each band was normalized against the internal standard analyzed on each blot (monoclonal antibodies anti-human histone 3 or glucose-6P-dehydrogenase were also from Santa Cruz).

Expression of results and statistical analyses

Data are presented as the means ± SD for the indicated number of experiments. Statistical analyses were performed using Student's *t* test, and *p* values < 0.05 were considered significant.

Results

Effects of stilbenes on acute UVB radiation-induced skin damage

The effectiveness of the topical treatment with stilbenes was first assayed using an acute proinflammatory UVB dose (360 mJ/cm², which is 2 × the minimal erythemal dose of UVB in albino hairless mice [24]) applied as a single dose 20 min before or after treatment with empty, Pter, or Resv liposomes. As shown in Fig. 1, control mice exposed to this acute dose of UVB radiation display physical/visible alterations: an increase in skin fold and thickness (Fig. 1A and B) and skin redness (Fig. 1C). The increase in these inflammation-related parameters was minimized in mice topically treated with Pter or Resv liposomes (Fig. 1A, B, and C). The protective effect was significantly better when the stilbenes were applied before than after the UVB irradiation (Fig. 1A and B). Thus for further experiments liposome administration was always performed before UVB irradiation.

Moreover, with an acute UVB irradiation, visibly, the skin wrinkled (Fig. 1C) and a subsequent and evident hyperplasia was observed in the histological stains (Fig. 1D) (both classical parameters related to photoaging). As shown in Fig. 1A, C, and D, Pter exerted a better protection than Resv. Transepidermal water loss (TEWL, measured by standard evaporimetry), which reflects skin barrier function, also increased in UVB (acute dose)-treated mice: $18 \pm 3 \text{ g/m}^2 \times \text{h}$ 24 h after UVB irradiation (versus $8 \pm 2 \text{ g/m}^2 \times \text{h}$ in control nonirradiated mice) ($n=7$ in both cases, $p < 0.01$). TEWL values obtained in mice treated with Pter or Resv and UVB (as in Fig. 1) were not significantly different from those measured in control nonirradiated mice.

Pterostilbene, but not resveratrol, prevents chronic UVB radiation-induced carcinogenesis

It is well known that UV radiation causes reactive oxygen species (ROS)-mediated oxidative stress [31]. We analyzed the antioxidant activities of Pter and Resv, which were similar in a cell-free standard assay (Fig. 2A). However, we observed that pretreatment of the skin with Pter resulted in a dramatic reduction in UVB-induced skin tumorigenesis (90% tumor-free mice at the end of treatment on the 40th week; $n=20$), whereas all Resv-treated mice showed carcinomas (0% tumor-free mice; $n=20$) (Fig. 2B, C, and D). On the 40th week the number of macroscopic skin carcinomas (of different sizes, see Fig. 2B) counted in Resv- and UVB-treated mice was always > 10, whereas the number of carcinomas found in 2 ($n=20$, 10%) Pter- and UVB-treated mice was just 1. Skin carcinomas were associated with strong hyperplasia and immune cell infiltration (Fig. 2C). After

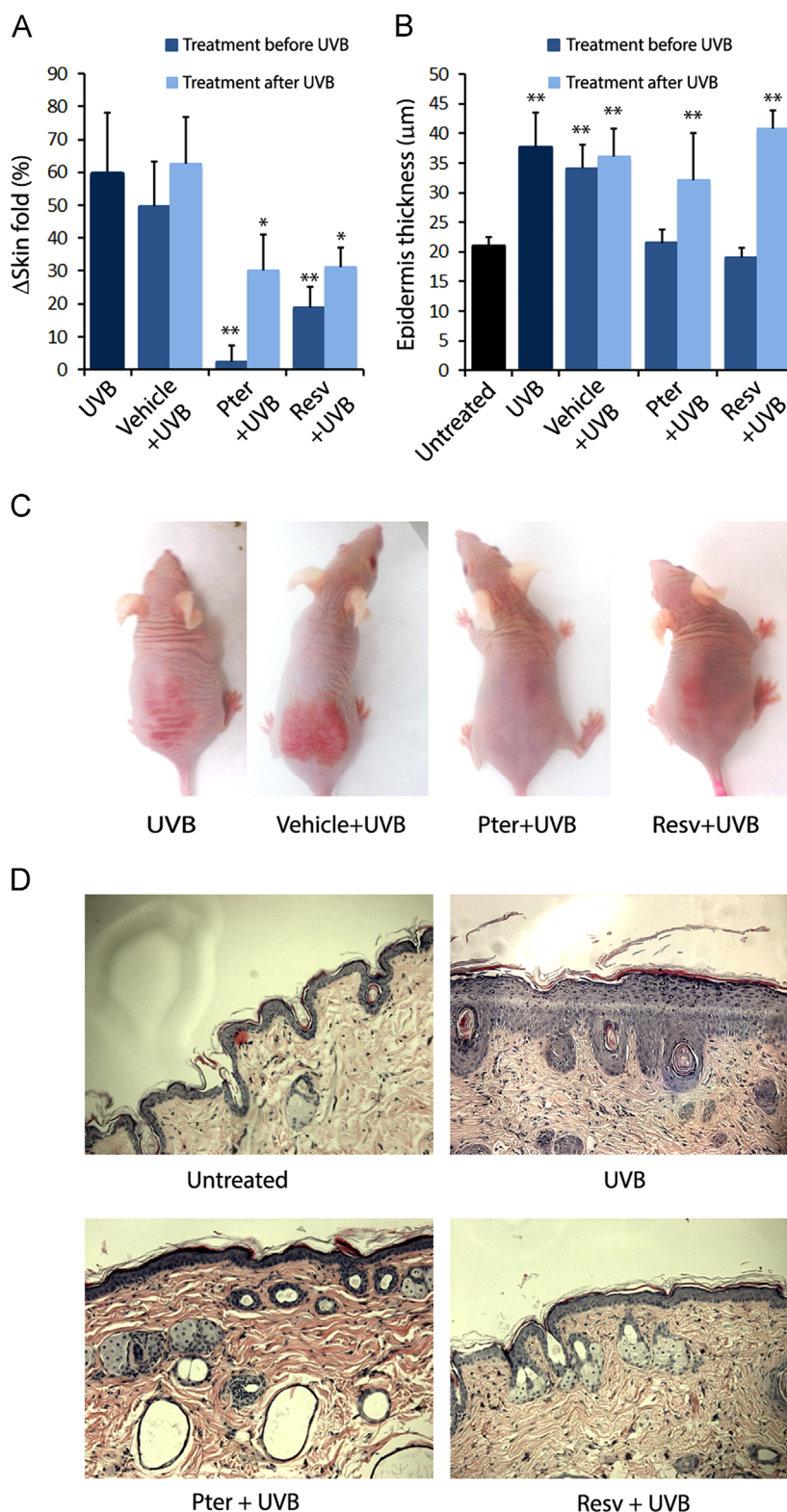


Fig. 1. Effects of pterostilbene and resveratrol on the protection of skin against acute proinflammatory UVB radiation. Mice received a single UVB radiation dose of 360 mJ/cm². (A) Skin fold (measured with calipers 24 h after UVB irradiation) in control (untreated) and UVB-treated mice (\pm empty liposomes, Pter liposomes, or Resv liposomes; 1 μ mol of each stilbene/cm² 20 min before or after irradiation); $n=10$, * $p < 0.05$ and ** $p < 0.01$ comparing all groups versus control untreated mice. (B) Epidermal thickness in control (untreated) and UVB-treated (\pm stilbenes, as in (A)) mice 1 week after UVB administration; $n=10$, ** $p < 0.01$. (C) Pictures showing UVB-induced skin redness 1 week after UVB administration. (D) Hematoxylin–eosin staining of skin samples obtained from control (untreated) and UVB-treated (1 week after UVB administration) (\pm stilbenes, as in (A)) mice. For (C) and (D), representative pictures of $n=10$ different mice/preparations per group are shown. Data shown for control untreated mice were not significantly different from those obtained in nonirradiated mice treated with empty liposomes, Pter liposomes, or Resv liposomes (not shown).

the treatment finished (180 days) none of the tumor-free Pter- and UVB-treated mice developed skin carcinomas within a posttreatment period of 3–4 months.

Molecular mechanisms involved in this strong anticancer effect elicited by Pter, compared with Resv, suggest differences that may be related to UVB absorption, prevention of DNA oxidation and

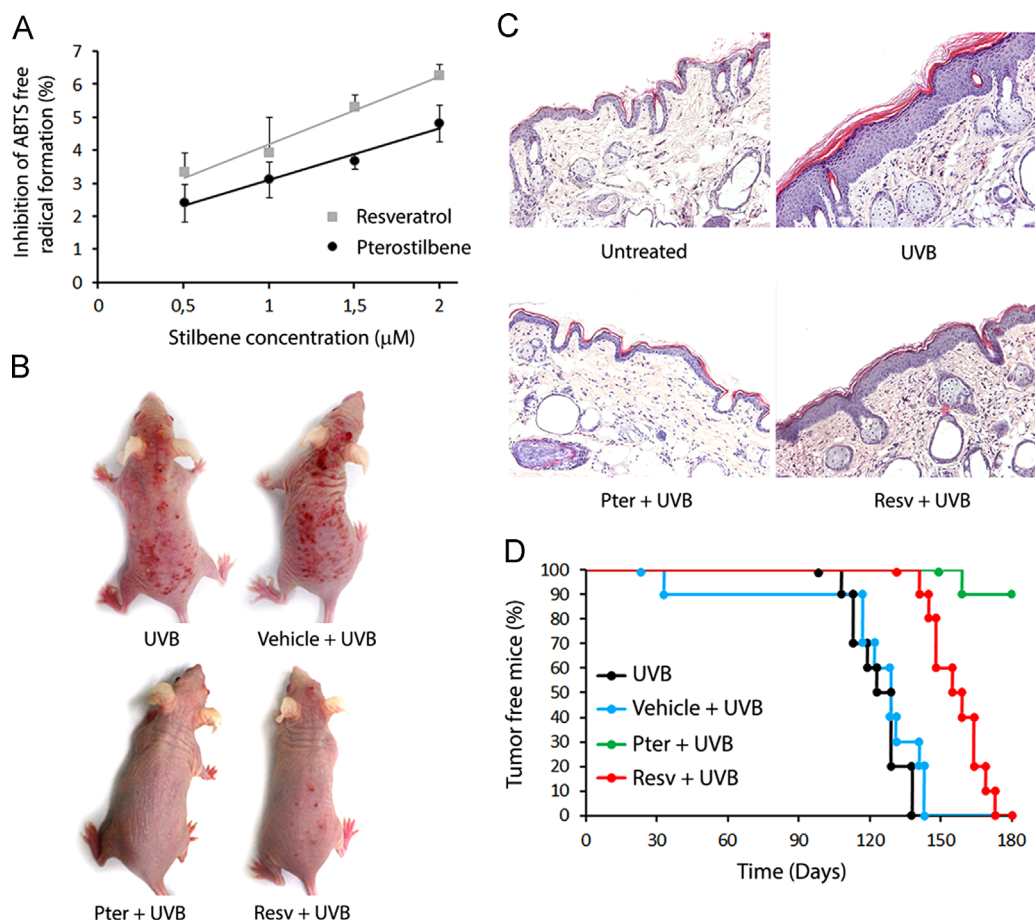


Fig. 2. Protective effects of pterostilbene and resveratrol against UVB-induced formation of cutaneous carcinomas. For carcinogenesis studies mice received, as indicated under Materials and methods, chronic UVB irradiation (180 mJ/cm^2 , three doses/week for 40 weeks) with or without stilbenes ($1 \mu\text{mol/cm}^2$ 20 min before each UVB irradiation). (A) Free radical-scavenging effect of stilbenes in a cell-free assay (Trolox) ($n=5$). (B) Control (untreated) and UVB radiation-treated mice (\pm empty liposomes, Pter liposomes, or Resv liposomes) (week 30). (C) Histology (week 24). Hematoxylin–eosin staining of skin samples obtained from control (untreated) and UVB radiation-treated mice (\pm empty liposomes, Pter liposomes, or Resv liposomes). Skin carcinomas associate with strong hyperplasia and immune cell infiltration. For (B) and (C), representative pictures of $n=20$ different preparations/mice per group are shown. (D) Tumor incidence (% of tumor-free mice) ($n=20$). Data shown for control untreated mice were not significantly different from those obtained in nonirradiated mice treated with empty liposomes, Pter liposomes, or Resv liposomes (not shown).

mutagenesis, protein and lipid oxidation, altered transcription and signaling mechanisms, and/or induction of cancer cell death.

First, we found differences between Pter and Resv regarding the UV absorption spectra (Fig. 3); however, the calculated SPF values (based on a scale from 0 to 50; see Materials and methods) were so low (Pter SPF was 2.95 ± 0.37 and Resv SPF 3.60 ± 0.42) that a direct physical effect cannot be responsible for the skin protection against UVB elicited by the stilbenes. Nevertheless Masaki et al. [32] showed that UVB-irradiated skin fibroblasts produce H_2O_2 , which leads to the formation of hydroxyl radicals, probably derived from the Fenton-like reaction ($\text{H}_2\text{O}_2 + \text{Fe}^{2+} \rightarrow \cdot\text{OH} + \text{OH}^- + \text{Fe}^{3+}$), which in turn damages the cells. In fact, because it has been shown that exposure of skin cells to, e.g., UVA induces an immediate release of labile iron [33], this mechanism could be (at least in part) responsible of the inflammatory and oxidative damages reported here. Therefore the photoprotective effects elicited by polyphenolic phytochemicals could involve, as previously suggested, potential iron-chelating effects (see, e.g., [34]). To evaluate this possibility we used two different strong iron chelators, desferrioxamine (DFO) and deferiprone (DFP), to investigate the possible participation of $\cdot\text{OH}$ in UVB-induced skin cell injury. For this purpose mice were pretreated (24 h before acute UVB irradiation) with DFO or DFP (150 nmol/cm^2 of skin; dissolved in physiological saline and 0.5% Carbopol) (these doses are high enough to ensure a fully effective removal of mouse skin labile iron (see, e.g., [35])). DFO and DFP significantly decreased by 44 ± 8 and $30 \pm 8\%$, respectively, the acute

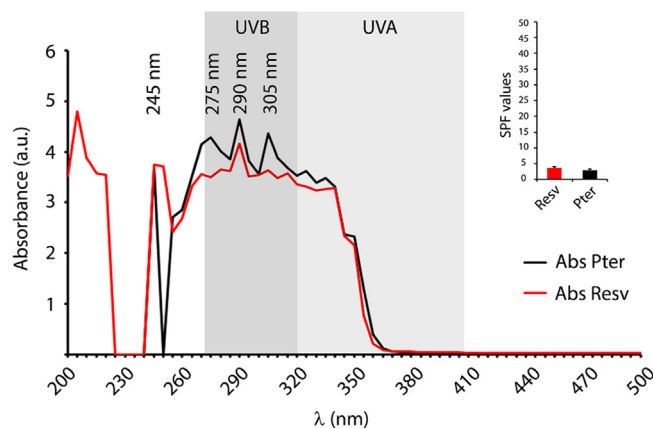


Fig. 3. UV absorbance spectra and sun protection factors for pterostilbene and resveratrol. SPF values ($n=5$ in each case) refer to a scale from 0 to 50 as indicated under Materials and methods (a.u., arbitrary units).

UVB (360 mJ/cm^2)-induced skin edema (% skin fold as in Fig. 1). Similar data were obtained for epidermal thickness (data not shown). Shorter protection times (e.g., 20 min or 12 h before UVB) or higher doses of chelators (up to 750 nmol/cm^2 of skin) did not render better results (not shown). However, resveratrol or pterostilbene (assayed using methodology to measure free iron—see

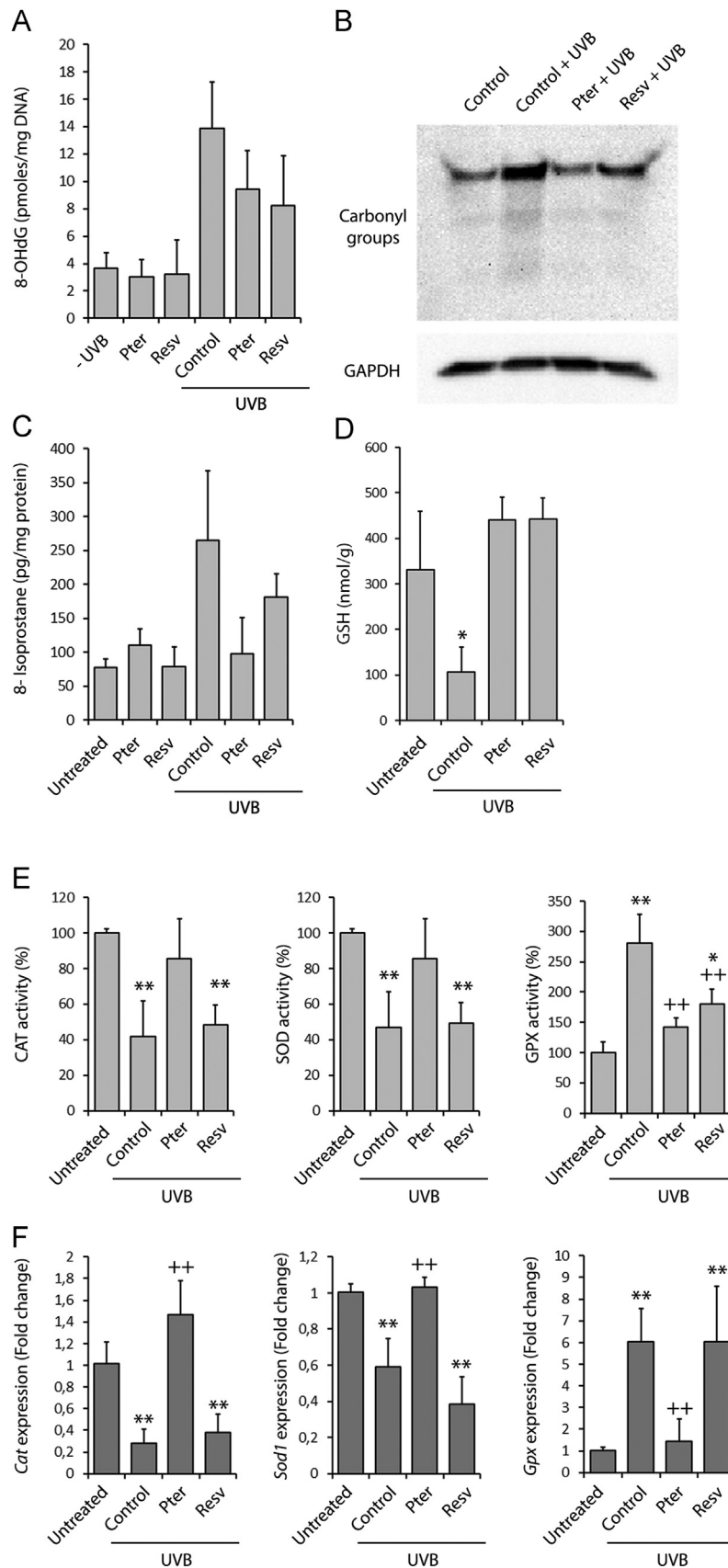


Fig. 4. Effects of stilbenes on the oxidation of DNA, proteins, and lipids and on different antioxidant enzyme activities in mice receiving chronic UVB irradiation. (A) 8-Hydroxy-2'-deoxyguanosine. (B) Protein carbonyls. (C) Isoprostanes. (D) GSH levels (relative to the number of epidermal cell layers). (E) Catalase, superoxide dismutase, and glutathione peroxidase activities (expressed as a % of control untreated mice). (F) RT-PCR for the indicated enzymes (fold change for control untreated mice is given a value of 1). All parameters were measured in skin samples obtained from control (untreated) and UVB radiation-treated mice (\pm empty liposomes, Pter liposomes, or Resv liposomes). Mice received UVB (180 mJ/cm², three doses/week for 30 weeks) and/or stilbenes (1 μ mol/cm² 20 min before each UVB irradiation); $n=10$, * $p < 0.05$ and ** $p < 0.01$ comparing each value versus controls (untreated mice); ++ $p < 0.01$ comparing Pter and UVB- or Resv and UVB-treated mice versus controls treated only with UVB. Data shown for control untreated mice were not significantly different from those obtained in nonirradiated mice treated with empty liposomes, Pter liposomes, or Resv liposomes (not shown).

Materials and methods) showed no detectable iron-chelating activity (whereas, e.g., DFO, in the absence or presence of resveratrol or pterostilbene, fully chelated free iron when incubated at equimolar

concentrations; not shown). This experimental evidence is in agreement with Miura et al. [36], who already found that changes in the spectrum of resveratrol and diethylstilbestrol did not occur by ferric or ferrous ions, suggesting that resveratrol and diethylstilbestrol do not produce a chelator with iron. Thus our data together suggest that the photoprotective effect elicited by Pter must necessarily involve a biological mechanism. Therefore, in the next experimental step, we focused on studying whether Pter and Resv prevent UVB-induced DNA, protein, and/or lipid oxidation and whether this is related to modulation of the skin antioxidant systems.

Pterostilbene decreases oxidative damage induced by chronic UVB radiation in the skin

As shown in Fig. 4 (where different biomarkers were used, e.g., [37]), Pter decreased chronic UVB-induced oxidative damage to DNA (8-hydroxy-2'-deoxyguanosine, a major mutagenic oxidative DNA lesion; Fig. 4A), proteins (protein carbonyls, which can result from oxidative cleavage of the protein backbone, direct oxidation of various amino acids, or the binding of aldehydes produced from lipid peroxidation; Fig. 4B), and lipids (isoprostanes, prostaglandin-like compounds formed in vivo from the free radical-catalyzed peroxidation of essential fatty acids; Fig. 4C). Pter also maintains a high (close to physiological) GSH level (a major cell antioxidant; Fig. 4D). In coordination with these effects, Pter also prevented the UVB-associated decrease in various key oxidative stress-related enzyme activities: CAT, SOD, and GPX (Fig. 4E). Moreover, enzyme activities measured in untreated and UVB-treated mice (\pm stilbenes) showed good correlation with their expression rates (RT-PCR) (Fig. 4F). Therefore it seems evident that Pter-induced photoprotection against deleterious UVB radiations involves modulation of skin antioxidant defenses. In this regard Pter, compared with Resv, showed a significantly better photoprotective effect on the antioxidant defenses; however, this was not reflected by significant differences in

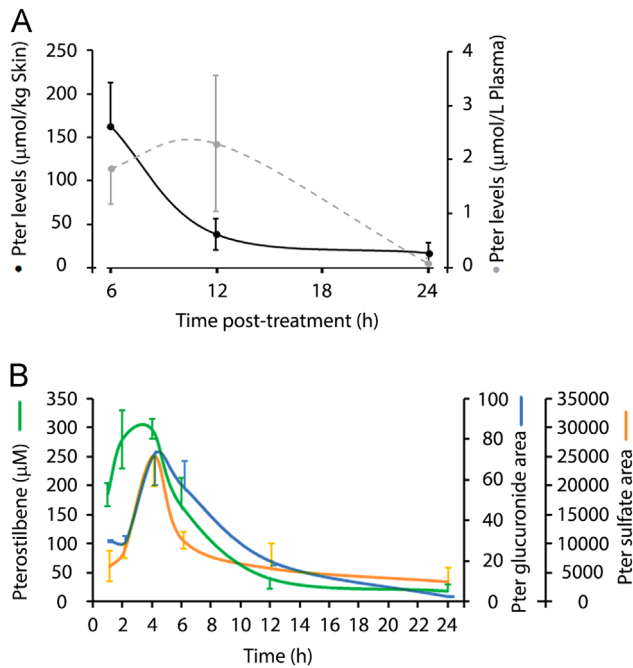


Fig. 5. Pterostilbene and its metabolites in the skin and plasma of mice. (A) Pter levels in plasma and the skin at various times after administration of Pter ($1 \mu\text{mol}/\text{cm}^2$) to nonirradiated mice; $n=5$. (B) Determination of Pter and its metabolites in the skin of nonirradiated mice at various times after administration of Pter ($1 \mu\text{mol}/\text{cm}^2$). The area calculated for Pter sulfate and Pter glucuronide directly reflects their skin concentration; however, a precise calculation was not possible because appropriate standards were not available.

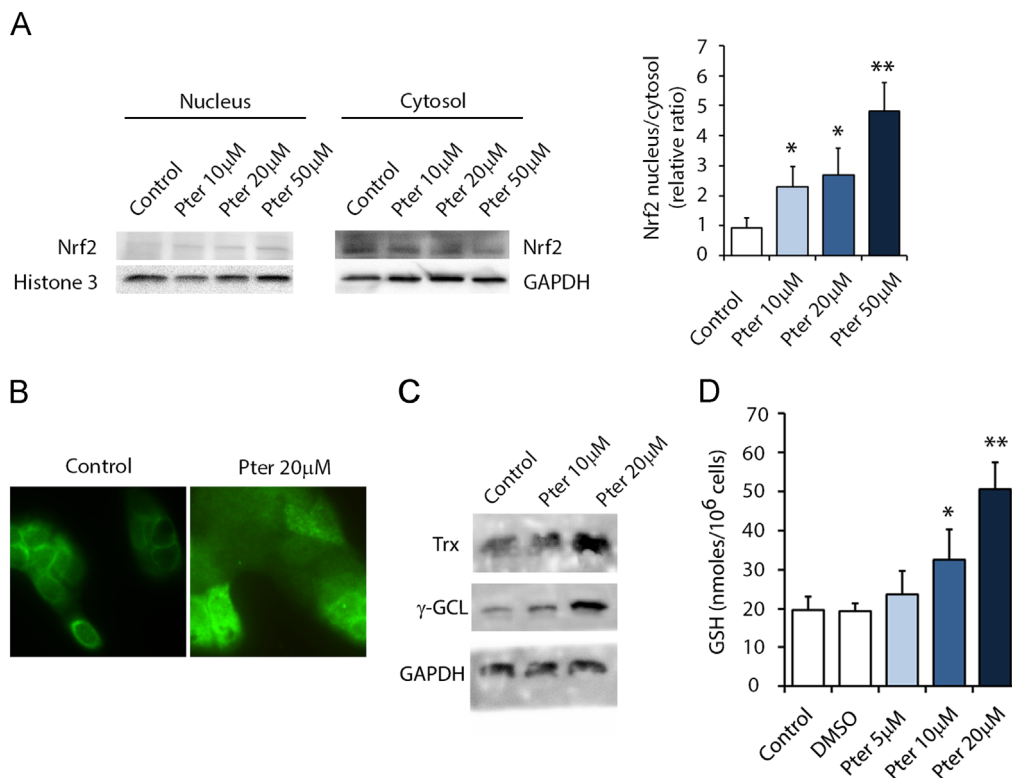


Fig. 6. Pterostilbene promotes Nrf2 activation in HaCat cells. Pter was added to cultured HaCat cells 24 h after seeding. Nrf2 detection by (A) Western blot and (B) immunostaining and (C) Trx and γ -GCL analysis by Western blot were performed 6 h after Pter addition. (D) GSH determination was performed 24 h after Pter addition. $*p < 0.05$ and $**p < 0.01$ comparing each value versus controls ($n=5$ in all conditions).

the levels of the oxidative damage biomarkers analyzed. Nevertheless, as discussed later, differences in the photoprotective effects of Pter and Resv may link intracellular (oxidative stress-related) signaling mechanisms and rates of UVB-induced mutagenesis.

Pterostilbene metabolism and bioavailability in the skin and the antioxidant response via nuclear factor erythroid-2-related factor-2 (Nrf2)

Nrf2 regulates the basal and inducible expression of a wide array of antioxidant and phase II enzyme genes (i.e., CAT, SOD, GPX, heme oxygenase-1, NAD(P)H quinone oxidoreductase, and γ -glutamyl-cysteine ligase). After dissociation from the cytosolic protein Keap1, a scaffolding protein that binds Nrf2 and Cul3 ubiquitin ligase for proteasome degradation, Nrf2 rapidly accumulates in the nucleus and transactivates the antioxidant response element (ARE) in the promoter region of target genes [38]. Thus we investigated the potential role of Nrf2, as a master regulator of the antioxidant response, in the protection of skin cells against UVB-induced damage. The keratinocyte is the predominant cell type in the epidermis, the outermost layer of the skin, constituting 90% of the cells found there. Thus we used HaCaT human keratinocytes, classically utilized for their high capacity to differentiate and proliferate in vitro, to assay this hypothesis.

To approach in vivo conditions in the in vitro setup, first we measured Pter levels in the skin after its topical administration. Pter levels in skin and plasma remained in the high micromolar range after topical 1 $\mu\text{mol}/\text{cm}^2$ Pter administration. Mean values for Pter in the skin were approximately 150 $\mu\text{mol}/\text{kg}$ (wet weight) within the first 6 h after topical administration (Fig. 5A). As shown in Fig. 5B, after topical administration of Pter, Pter-sulfate and Pter-glucuronide (main Pter-derived metabolites generated under in vivo conditions [39]) increased in the skin. Using pooled human liver microsomes, it was shown that glucuronidation of Pter is much less efficient than that of Resv, thus suggesting that Pter may have decreased metabolism in humans [19], a fact in favor of the higher bioavailability of Pter versus that of Resv. Nevertheless, this conclusion was premature and misleading because Azzolini et al. [39] later demonstrated that the main in vivo-generated Pter metabolite is Pter-sulfate.

For in vitro experiments we used Pter and not its metabolites because it has been repeatedly shown that natural Pter is biologically more active than its metabolites [11]. As shown in Fig. 6A Nrf2 translocation into the nucleus increases as the concentration of added Pter increases (within the range of Pter bioavailability in the skin) in cultured HaCaT cells. Western blots were confirmed by Nrf2 immunostaining (Fig. 6B) showing an increased nuclear Nrf2-linked fluorescence in the presence of Pter. In agreement with the Pter-induced increase in nuclear Nrf2, increased expression of some Nrf2-dependent molecules was also detected in the presence of Pter (γ -GCL, Trx; Fig. 6C). Moreover, in agreement with the Pter-induced increase in γ -GCL, a consequent increase in intracellular GSH levels was also observed (Fig. 6D), thus suggesting a close relationship between the photoprotective effect elicited by Pter and its capacity to modulate the Nrf2-dependent antioxidant response. Nevertheless the molecular mechanisms underlying the observed differences between Pter and Resv, as well as the potent photoprotective effect elicited by Pter, remain open questions that need further investigation.

Discussion

Epidemiological studies indicate that solar UV radiation is mainly responsible for skin tumor development and photoaging [2]. Exposure of the skin to solar UV radiation results in

inflammation, oxidative stress, direct and ROS-mediated DNA damage, dysregulation of cellular signaling pathways, and immunosuppression, which promote skin cancer [2]. Polyphenolic phytochemicals, possessing anti-inflammatory, immunomodulatory, and antioxidant properties, are among the most promising group of compounds that can be exploited as chemopreventive/therapeutic agents for a variety of skin disorders, including skin cancer [40]. Indeed potential anticancer/photoprotective properties have been suggested for various polyphenols, including, e.g., green tea polyphenols, grape seed proanthocyanidins, Resv, silymarin, luteolin, and genistein [41]. For example, and despite having a minimum SPF, tea extract (containing epigallocatechin-3-gallate) has protective effects against DNA damage and UV-induced immunosuppression (partly because of its ability to reduce oxidative stress, inhibit NF- κ B, and facilitate repair of DNA damage) [42–44].

In addition it has been shown that Pter is as potent as Resv in inhibiting 12-O-tetradecanoylphorbol-13-acetate (TPA) activated NF- κ B, AP-1, COX-2, and iNOS in mouse epidermis [45] and that Pter potentially inhibits 7,12-dimethylbenz[*a*]anthracene/TPA-induced mouse skin carcinogenesis [46]. As shown in the present article Pter is clearly superior to Resv in preventing acute and chronic UVB radiation-induced skin damage. As shown in Fig. 2D, Resv was unable to exert protection (50% of Resv-treated mice developed skin carcinomas by week 21, and 100% by week 30). Other polyphenols used with the same protocol (including curcumin, EGCG, epicatechin, apigenin, genistein, ellagic acid, or lutein) did not render better results than Resv [21]. Moreover, topical administration of Pter (at effective doses) does not cause any apparent skin toxicity (as suggested by comparing the histological features of control untreated mice or Pter-treated mice receiving chronic UVB radiations). As shown in Fig. 2B, skin of chronic UVB radiation- and Pter-treated mice appears to have the same healthy aspect as that of control untreated mice. This lack of apparent cutaneous toxicity also seems coherent with a previous study in which mice fed for 28 days at doses of 0, 30, 300, and 3000 mg/kg body wt/day of Pter showed that the red blood cell number and hematocrit increased after Pter administration compared to control groups; as well, histopathologic examination and evaluation of biochemical parameters revealed no alterations regarding clinical signs or organ weight at any dose [47]. No mortality was observed even with the highest dose administered with the food [47].

The photoprotective effect elicited by Pter, as suggested by its minimum SPF (Fig. 3) and the absence of iron-chelating activity (see Results), must be fundamentally biological. In this sense various mechanisms and cellular targets of photoprotection by bioactive polyphenols have been proposed, i.e., modulation of cellular signaling pathways (e.g., activation of NF- κ B and members of the AP-1 complex, MAPKs, PI3K/Akt, and STAT3), anti-inflammatory/anti-immunosuppression activities, or enhancement of nucleotide excision repair genes (see [48] for an excellent review). Our present results show that Pter decreases UVB-induced oxidative damage and upregulates a group of antioxidant enzyme activities (Fig. 4). Topical administration facilitates the use of high doses of Pter; therefore it is plausible that part of this photoprotection is due to direct antioxidant effects. In addition, the absence of hyperplasia and inflammatory cell infiltration in UVB- and Pter-treated mice, compared to UVB-treated mice (Figs. 1D and 2C), also supports the known anti-inflammatory/anti-immunosuppressive activity of polyphenols. Nevertheless the effect of Pter in preventing the UVB-induced decrease of antioxidant enzyme activities and GSH also suggests an additional mechanism.

ROS can promote tumor initiation by damaging DNA that will lead to mutations and by augmenting signaling pathways that promote cell growth and proliferation [49]. NF- κ B, AP-1, and

MAPK induction or STAT3 tyrosine phosphorylation are all triggered by oxidative stress [50]; therefore control of ROS levels seems a primary mechanism by which Pter could be particularly effective. In this work we focused on Nrf2 signaling as a possible mechanism because the Keap1–Nrf2–ARE pathway is known to control the oxidative stress response [51]. The mechanism of Nrf2 activation by polyphenols ultimately results in the disruption of the Keap1–Nrf2 complex, probably through interaction with the thiols present on Keap1. This interaction may involve thiol modification either by direct alkylation or by oxidation to the disulfide form [52,53]. Previous reports indicate that, e.g., (a) Pter prevented azoxymethane-induced colon tumorigenesis, and the administration of Pter for 6 weeks significantly enhanced expression of antioxidant enzymes, such as heme oxygenase-1 and glutathione reductase, via activation of Nrf2 signaling [12]; (b) treatment of HaCaT keratinocytes with Resv resulted in increased nuclear localization of Nrf2, decrease in cytosolic Keap1, and protection against UVA-induced apoptosis [54]; (c) Pter induced significant activation of Nrf2, in a dose- and time-dependent manner, in streptozotocin-treated INS-1E rat pancreatic β cells [55]; and (d) in HeLa cells Pter triggered ER stress by redox homeostasis imbalance, which was negatively regulated by a following activation of Nrf2 [56]. Our results in HaCaT cells show that Pter increases Nrf2 translocation into the nucleus and expression of Nrf2-dependent (oxidative stress-related) molecules (Fig. 6), thus further supporting the idea, as previously suggested [57], that Nrf2 may be a central regulator of UV protection in the epidermis. Nevertheless conclusive results would benefit from using knockout mice, which experiments are now under way in our lab. In this sense our results also are in agreement with a previous report by Saw et al. [58] showing that Nrf2 deficiency (C57BL/6 mice) enhances UVB (a single dose of 300 mJ/cm²)-induced skin inflammation and extracellular matrix damage. Moreover, recent findings also indicate that the tumor suppressor activity of p53 is related to its role in maintaining cellular redox by regulating cellular metabolism [51]. For instance, using a p53-knockout model, it was demonstrated that lack of expression of some antioxidative stress proteins (i.e., Sestrin 1 and 2, GPX, and phosphate-activated mitochondrial glutaminase) is associated with increased cellular ROS, which leads to increases in DNA oxidation and in the mutation rate, thus promoting tumorigenesis [51,59]. Therefore possible Nrf2 and p53 coregulation, at the skin level, is a feasible mechanism that also deserves further study.

Finally, although Pter seems more potent than Resv in antioxidant activity and absorption rate, a highly extensive comparison has not been conducted [11]. Based on our present knowledge [11,41] (see also above) the following molecular targets/pathways should be explored in depth to establish mechanistic differences between both natural stilbenes: Nrf2 and possible p-53 and/or c-Myc coregulation, MAPKs, PI3K/Akt, STAT3, expression of nucleotide excision repair genes, cyclin D1/CDK4-dependent cell proliferation, apoptosis evasion, and angiogenesis.

Conclusions

Pter prevented acute UVB radiation-induced inflammation and photoaging-associated skin damage. Pter, but not Resv, effectively prevented chronic UVB radiation-induced skin carcinogenesis. The anticarcinogenic effect elicited by Pter was associated with maintenance of skin antioxidant defenses and inhibition of UVB-induced oxidative damages. Based on our present results we propose the use of Pter for the prevention of skin carcinogenesis induced by solar radiation.

Acknowledgments

This research was supported by the IMPIVA (Generalitat Valenciana, Spain; Grant SOLI1519880408JF27022009092842), the MINECO (Spain; Grant SAF2012–31565), and Green Molecular (Paterna, Spain). M.L.R. held a fellowship from the MICINN (Spain).

References

- [1] Berwick, M.; Lachiewicz, A.; Pestak, C.; Thomas, N. Solar UV exposure and mortality from skin tumors. *Adv. Exp. Med. Biol.* **624**:117–124; 2008.
- [2] Afaq, F.; Adhami, V. M.; Mukhtar, H. Photochemoprevention of ultraviolet B signaling and photocarcinogenesis. *Mutat. Res.* **571**:153–173; 2005.
- [3] Marrot, L.; Meunier, J. R. Skin DNA photodamage and its biological consequences. *J. Am. Acad. Dermatol.* **58**:S139–S148; 2008.
- [4] Yang, C. S.; Wang, X.; Lu, G.; Picinich, S. C. Cancer prevention by tea: animal studies, molecular mechanisms and human relevance. *Nat. Rev. Cancer* **9**:429–439; 2009.
- [5] Mukhtar, H.; Ahmad, N. Tea polyphenols: prevention of cancer and optimizing health. discussion 1703S–1694S. *Am. J. Clin. Nutr.* **71**:1698S–1702S; 2000.
- [6] Jou, P. C.; Tomecki, K. J. Sunscreens in the United States: current status and future outlook. *Adv. Exp. Med. Biol.* **810**:464–484; 2014.
- [7] Filip, A.; Clichici, S.; Daicovicu, D.; Adriana, M.; Postescu, I. D.; Perdeschrepler, M.; Olteanu, D. Photochemoprevention of cutaneous neoplasia through natural products. *Exp. Oncol.* **31**:9–15; 2009.
- [8] Korkina, L. G.; Pastore, S.; Dellambra, E.; De Luca, C. New molecular and cellular targets for chemoprevention and treatment of skin tumors by plant polyphenols: a critical review. *Curr. Med. Chem.* **20**:852–868; 2013.
- [9] Jang, M.; Cai, L.; Udeani, G. O.; Slowing, K. V.; Thomas, C. F.; Beecher, C. W.; Fong, H. H.; Farnsworth, N. R.; Kinghorn, A. D.; Mehta, R. G.; Moon, R. C.; Pezzuto, J. M. Cancer chemopreventive activity of resveratrol, a natural product derived from grapes. *Science* **275**:218–220; 1997.
- [10] Aziz, M. H.; Reagan-Shaw, S.; Wu, J.; Longley, B. J.; Ahmad, N. Chemoprevention of skin cancer by grape constituent resveratrol: relevance to human disease? *FASEB J* **19**:1193–1195; 2005.
- [11] Estrela, J. M.; Ortega, A.; Mena, S.; Rodriguez, M. L.; Asensi, M. Pterostilbene: biomedical applications. *Crit. Rev. Clin. Lab. Sci.* **50**:65–78; 2013.
- [12] Chiou, Y. S.; Tsai, M. L.; Nagabhushanam, K.; Wang, Y. J.; Wu, C. H.; Ho, C. T.; Pan, M. H. Pterostilbene is more potent than resveratrol in preventing azoxymethane (AOM)-induced colon tumorigenesis via activation of the NF-E2-related factor 2 (Nrf2)-mediated antioxidant signaling pathway. *J. Agric. Food Chem.* **59**:2725–2733; 2011.
- [13] Paul, S.; Rimando, A. M.; Lee, H. J.; Ji, Y.; Reddy, B. S.; Suh, N. Anti-inflammatory action of pterostilbene is mediated through the p38 mitogen-activated protein kinase pathway in colon cancer cells. *Cancer Prev. Res. (Philadelphia)* **2**:650–657; 2009.
- [14] Halliday, G. M. Inflammation, gene mutation and photoimmunosuppression in response to UVR-induced oxidative damage contributes to photocarcinogenesis. *Mutat. Res.* **571**:107–120; 2005.
- [15] Lin, H. S.; Yue, B. D.; Ho, P. C. Determination of pterostilbene in rat plasma by a simple HPLC-UV method and its application in pre-clinical pharmacokinetic study. *Biomed. Chromatogr.* **23**:1308–1315; 2009.
- [16] Kapetanovic, I. M.; Muzzio, M.; Huang, Z.; Thompson, T. N.; McCormick, D. L. Pharmacokinetics, oral bioavailability, and metabolic profile of resveratrol and its dimethylether analog, pterostilbene, in rats. *Cancer Chemother. Pharmacol.* **68**:593–601; 2011.
- [17] Remsberg, C. M.; Yanez, J. A.; Ohgami, Y.; Vega-Villa, K. R.; Rimando, A. M.; Davies, N. M. Pharmacometrics of pterostilbene: preclinical pharmacokinetics and metabolism, anticancer, anti-inflammatory, antioxidant and analgesic activity. *Phytother. Res.* **22**:169–179; 2008.
- [18] Yeo, S. C.; Ho, P. C.; Lin, H. S. Pharmacokinetics of pterostilbene in Sprague-Dawley rats: the impacts of aqueous solubility, fasting, dose escalation, and dosing route on bioavailability. *Mol. Nutr. Food Res.* **57**:1015–1025; 2013.
- [19] Dellinger, R. W.; Garcia, A. M.; Meyskens Jr. F. L. Differences in the glucuronidation of resveratrol and pterostilbene: altered enzyme specificity and potential gender differences. *Drug Metab. Pharmacokinet.* **29**:112–119; 2014.
- [20] Joseph, J. A.; Fisher, D. R.; Cheng, V.; Rimando, A. M.; Shukitt-Hale, B. Cellular and behavioral effects of stilbene resveratrol analogues: implications for reducing the deleterious effects of aging. *J. Agric. Food Chem.* **56**:10544–10551; 2008.
- [21] Estrela, J.; Asensi, M. Pterostilbene (pter) for use in the prevention and/or treatment of skin diseases, damages or injuries. S.L. (PCT/EP2010/066544). *Patent from Green Molecular* ; 2009.
- [22] Huang, D.; Ou, B.; Prior, R. L. The chemistry behind antioxidant capacity assays. *J. Agric. Food Chem.* **53**:1841–1856; 2005.
- [23] Diffey, B.; Robson, J. A new substrate to measure sunscreen protection factors throughout the ultraviolet spectrum. *J. Soc. Cosmet. Chem.* **40**:127–133; 1989.
- [24] Tan, E. M.; Freeman, R. G.; Stoughton, R. B. Action spectrum of ultraviolet light-induced damage to nuclear DNA in vivo. *J. Invest. Dermatol.* **55**:439–443; 1970.
- [25] Sharma, S.D.; Katiyar, S.K. Dietary grape seed proanthocyanidins inhibit UVB-induced cyclooxygenase-2 expression and other inflammatory mediators in UVB-exposed skin and skin tumors of SKH-1 hairless mice. *Pharm. Res.* **27**:1092–1102.

- [26] Matsumoto, K.; Mizukoshi, K.; Oyobikawa, M.; Ohshima, H.; Sakai, Y.; Tagami, H. Objective evaluation of the efficacy of daily topical applications of cosmetics bases using the hairless mouse model of atopic dermatitis. *Skin Res. Technol.* **11**:209–217; 2005.
- [27] Ferrer, P.; Asensi, M.; Segarra, R.; Ortega, A.; Benlloch, M.; Obrador, E.; Varea, M. T.; Asensio, G.; Jorda, L.; Estrela, J. M. Association between pterostilbene and quercetin inhibits metastatic activity of B16 melanoma. *Neoplasia* **7**:37–47; 2005.
- [28] Escobar, J.; Cubells, E.; Enomoto, M.; Quintas, G.; Kuligowski, J.; Fernandez, C. M.; Torres-Cuevas, I.; Sastre, J.; Belik, J.; Vento, M. Prolonging in utero-like oxygenation after birth diminishes oxidative stress in the lung and brain of mice pups. *Redox Biol.* **1**:297–303; 2013.
- [29] Crain, P. F. Preparation and enzymatic hydrolysis of DNA and RNA for mass spectrometry. *Methods Enzymol.* **193**:782–790; 1990.
- [30] Kumar, A.; Singh, C. K.; Lavoie, H. A.; Dipette, D. J.; Singh, U. S. Resveratrol restores Nrf2 level and prevents ethanol-induced toxic effects in the cerebellum of a rodent model of fetal alcohol spectrum disorders. *Mol. Pharmacol.* **80**:446–457; 2011.
- [31] Sander, C. S.; Chang, H.; Hamm, F.; Elsner, P.; Thiele, J. J. Role of oxidative stress and the antioxidant network in cutaneous carcinogenesis. *Int. J. Dermatol.* **43**:326–335; 2004.
- [32] Masaki, H.; Atsumi, T.; Sakurai, H. Detection of hydrogen peroxide and hydroxyl radicals in murine skin fibroblasts under UVB irradiation. *Biochem. Biophys. Res. Commun.* **206**:474–479; 1995.
- [33] Reelfs, O.; Tyrrell, R. M.; Pourzand, C. Ultraviolet A radiation-induced immediate iron release is a key modulator of the activation of NF-kappaB in human skin fibroblasts. *J. Invest. Dermatol.* **122**:1440–1447; 2004.
- [34] Li, Y.; Deng, Y.; Tang, Y.; Yu, H.; Gao, C.; Liu, L.; Yao, P. Quercetin protects rat hepatocytes from oxidative damage induced by ethanol and iron by maintaining intercellular labile iron pool. *Hum. Exp. Toxicol.* **33**:534–541; 2014.
- [35] Soybir, G. R.; Koyuncu, H.; Koksoy, F.; Yalcin, O.; Ozseker, A.; Alatlci, C.; Topuzlu, C. Protective effect of desferrioxamin against TPA caused inflammation in CD-1 mouse skin. *Surg. Oncol.* **5**:253–258; 1996.
- [36] Miura, T.; Muraoka, S.; Ikeda, N.; Watanabe, M.; Fujimoto, Y. Antioxidative and prooxidative action of stilbene derivatives. *Pharmacol. Toxicol.* **86**:203–208; 2000.
- [37] Tucker, P. S.; Dalbo, V. J.; Han, T.; Kingsley, M. I. Clinical and research markers of oxidative stress in chronic kidney disease. *Biomarkers* **18**:103–115; 2013.
- [38] Pervaiz, S.; Holme, A. L. Resveratrol: its biologic targets and functional activity. *Antioxid. Redox Signaling* **11**:2851–2897; 2009.
- [39] Azzolini, M.; La Spina, M.; Mattarei, A.; Paradisi, C.; Zoratti, M.; Biasutto, L. Pharmacokinetics and tissue distribution of pterostilbene in the rat. *Mol. Nutr. Food Res.* **58**:2122–2132; 2014.
- [40] Asensi, M.; Ortega, A.; Mena, S.; Feddi, F.; Estrela, J. M. Natural polyphenols in cancer therapy. *Crit. Rev. Clin. Lab. Sci.* **48**:197–216; 2011.
- [41] Nichols, J. A.; Katiyar, S. K. Skin photoprotection by natural polyphenols: anti-inflammatory, antioxidant and DNA repair mechanisms. *Arch. Dermatol. Res.* **302**:71–83; 2010.
- [42] Morley, N.; Clifford, T.; Salter, L.; Campbell, S.; Gould, D.; Curnow, A. The green tea polyphenol (–)-epigallocatechin gallate and green tea can protect human cellular DNA from ultraviolet and visible radiation-induced damage. *Photo-dermatol. Photoimmunol. Photomed.* **21**:15–22; 2005.
- [43] Matsui, M. S.; Hsia, A.; Miller, J. D.; Hanneman, K.; Scull, H.; Cooper, K. D.; Baron, E. Non-sunscreen photoprotection: antioxidants add value to a sunscreen. *J. Invest. Dermatol. Symp. Proc.* **14**:56–59; 2009.
- [44] Katiyar, S. K. Green tea prevents non-melanoma skin cancer by enhancing DNA repair. *Arch. Biochem. Biophys.* **508**:152–158; 2011.
- [45] Cichocki, M.; Paluszczak, J.; Szafer, H.; Piechowiak, A.; Rimando, A. M.; Baer-Dubowska, W. Pterostilbene is equally potent as resveratrol in inhibiting 12-O-tetradecanoylphorbol-13-acetate activated NFkappaB, AP-1, COX-2, and iNOS in mouse epidermis. *Mol. Nutr. Food Res.* **52**(Suppl. 1):S62–S70; 2008.
- [46] Tsai, M. L.; Lai, C. S.; Chang, Y. H.; Chen, W. J.; Ho, C. T.; Pan, M. H. Pterostilbene, a natural analogue of resveratrol, potently inhibits 7,12-dimethylbenz[a]anthracene (DMBA)/12-O-tetradecanoylphorbol-13-acetate (TPA)-induced mouse skin carcinogenesis. *Food Funct.* **3**:1185–1194; 2012.
- [47] Ruiz, M. J.; Fernandez, M.; Pico, Y.; Manes, J.; Asensi, M.; Carda, C.; Asensio, G.; Estrela, J. M. Dietary administration of high doses of pterostilbene and quercetin to mice is not toxic. *J. Agric. Food Chem.* **57**:3180–3186; 2009.
- [48] Afaq, F.; Katiyar, S. K. Polyphenols: skin photoprotection and inhibition of photocarcinogenesis. *Mini Rev. Med. Chem.* **11**:1200–1215; 2011.
- [49] Ray, P. D.; Huang, B. W.; Tsuji, Y. Reactive oxygen species (ROS) homeostasis and redox regulation in cellular signaling. *Cell. Signalling* **24**:981–990; 2012.
- [50] Bito, T.; Nishigori, C. Impact of reactive oxygen species on keratinocyte signaling pathways. *J. Dermatol. Sci.* **68**:3–8; 2012.
- [51] Rotblat, B.; Melino, G.; Knight, R. A. NRF2 and p53: Januses in cancer? *Oncotarget* **3**:1272–1283; 2012.
- [52] Lee-Hilz, Y. Y.; Boerboom, A. M.; Westphal, A. H.; Berkel, W. J.; Aarts, J. M.; Rietjens, I. M. Pro-oxidant activity of flavonoids induces EpRE-mediated gene expression. *Chem. Res. Toxicol.* **19**:1499–1505; 2006.
- [53] Bensasson, R. V.; Zoete, V.; Dinkova-Kostova, A. T.; Talalay, P. Two-step mechanism of induction of the gene expression of a prototypic cancer-protective enzyme by diphenols. *Chem. Res. Toxicol.* **21**:805–812; 2008.
- [54] Liu, Y.; Chan, F.; Sun, H.; Yan, J.; Fan, D.; Zhao, D.; Zhou, J. D. Resveratrol protects human keratinocytes HaCaT cells from UVA-induced oxidative stress damage by downregulating Keap1 expression. *Eur. J. Pharmacol.* **650**:130–137; 2011.
- [55] Bhakkiyalakshmi, E.; Shalini, D.; Sekar, T. V.; Rajaguru, P.; Paulmurugan, R.; Ramkumar, K. M. Therapeutic potential of pterostilbene against pancreatic beta-cell apoptosis mediated through Nrf2. *Br. J. Pharmacol.* **171**:1747–1757; 2014.
- [56] Zhang, B.; Wang, X. Q.; Chen, H. Y.; Liu, B. H. Involvement of the Nrf2 pathway in the regulation of pterostilbene-induced apoptosis in HeLa Cells via ER stress. *J. Pharmacol. Sci.* **126**:216–229; 2014.
- [57] Schafer, M.; Dutsch, S.; auf dem Keller, U.; Werner, S. Nrf2: a central regulator of UV protection in the epidermis. *Cell Cycle* **9**:2917–2918; 2010.
- [58] Saw, C. L.; Yang, A. Y.; Huang, M. T.; Liu, Y.; Lee, J. H.; Khor, T. O.; Su, Z. Y.; Shu, L.; Lu, Y.; Conney, A. H.; Kong, A. N. Nrf2 null enhances UVB-induced skin inflammation and extracellular matrix damages. *Cell Biosci* **4**:39; 2014.
- [59] Sablina, A. A.; Budanov, A. V.; Ilyinskaya, G. V.; Agapova, L. S.; Kravchenko, J. E.; Chumakov, P. M. The antioxidant function of the p53 tumor suppressor. *Nat. Med.* **11**:1306–1313; 2005.